Vibration analysis of cracked frame structures

Ahmed M. Ibrahim[1], Hasan Ozturk[*1] and Mustafa Sabuncu[2]

[1]*Mechanical Engineering Department, Dokuz Eylul University Buca, Izmir, Turkey*
[2]*The Graduate School of Natural and Applied Sciences, Dokuz Eylul University,
Tinaztepe, Buca, Izmir, Turkey*

Abstract. In this study, the effects of crack depth and crack location on the in-plane free vibration of cracked frame structures have been investigated numerically by using the Finite Element Method. For the rectangular cross-section beam, a crack element is developed by using the principles of fracture mechanics. The effects of crack depth and location on the natural frequency of multi-bay and multi-store frame structures are presented in 3D graphs. The comparison between the present work and the results obtained from ANSYS shows a very good agreement.

Keywords: cracked frame; free vibration; multi-bay; multi-story; finite element method

1. Introduction

In many applications, frame structures are widely used, for example in buildings, bridges and gas or steam turbine blade packets. Frames are also one of the structures in which static and dynamic problems generally occur. These frames are subjected to concentrated and distributed static or dynamic loads which may cause static (buckling) and dynamic instability. Moreover, the cracks can be seen in frame structures due to reasons like erosion, corrosion, fatigue or accidents. The presence of a crack can not only cause a local variation in the stiffness, but many also affect the mechanical behavior of the entire structure to a considerable extent.

Many investigations about the vibration and buckling (static stability) characteristics of frames of various types have been carried out. Syngellakis and Kameshki (1994) have studied the elastic critical loads for plane frames by using the transfer matrix method. Bayo and Loureiro (2001) have presented a direct one-step method, which is based on a non-linear analysis of the structure starting from an initial deformation state that includes the initial imperfections of the elements, for the buckling analysis of steel frame structures. Xu and Liu (2002) have developed a practical method for the stability analysis of semi-braced steel frames with the effect of semi-rigid behaviour of beam-to-column connections being taken into account. A simplified procedure for determining approximate values for the buckling loads of both regular and irregular frames was developed by Girgin *et al.* (2006); the procedure utilizes lateral load analysis of frames and yields errors on the order of 5%, which may be considered suitable for design purposes. Tong and Xing (2007) have studied the instability of braced frames by geometric and nonlinear material analysis accounting

---

*Corresponding author, Associate Professor, E-mail: hasan.ozturk@deu.edu.tr

for residual stresses, initial sway imperfection and member initial bow. In this study, the change in the buckling mode with increasing bracing stiffness was analyzed and the relationship between the ultimate load capacity and the bracing rigidity was developed. Trahair (2009) has studied the method of designing steel beams, columns, and plane frames against out-of-plane failure, which uses the results of an elastic flexural-torsional buckling analysis in the strength rules of design codes, which has been named design by buckling analysis (DBA). A general digital computer method based on a Sturm sequence procedure has been described by Gupta (1970) for determining the natural frequencies and associated modes of undamped free vibration of frames and other structures whose stiffness and mass matrices are of band form. Analytical and experimental investigations on vibrating frames carrying concentrated masses, and in-plane vibrations of portal frames with end supports, elastically restrained against rotation and translation, have been studied by using analytical solutions and the finite element method (Laurai 1987, Filipich 1987, 1989). Chang and Chang (1991) have examined free and forced out-of-plane vibrations of elastic plane frames using exact solutions of the Euler-Bernoulli equation for transversely vibrating beams coupled with torsional vibrations. The natural frequencies and mode shapes for the in-plane vibration of triangular closed and planar frames (portal, *H* and *T* frames) have been studied by using the Rayleigh-Ritz method (Lee 1993, Lee and Ng 1994).

Christides and Barr (1984) have derived the differential equation and associated boundary conditions for a nominally uniform Bernoulli-Euler beam containing one or more pairs of symmetric cracks. A surface crack on a beam section has introduced a local flexibility to the structural member on a study carried out by Gounaris and Dimarogonas (1988). In this study, a finite element model for a cracked prismatic beam has been developed. Qian *et al.* (1990) have derived an element stiffness matrix of a beam with a crack from an integration of stress intensity factors and established a finite element model of a cracked beam for a cantilever beam with an edge-crack. Chondros and Dimarogonas (1989) have used the Rayleigh principle for an estimation of the change in the natural frequencies and modes of vibration of the structure if the crack geometry is known. Ostachowicz and Krawczuk (1990) have studied the forced vibrations of the beam and the effects of the crack locations and sizes on the vibrational behavior of the structure and discussed a basis for crack identification. Lee and Ng (1994) have determined the natural frequencies and modes for the flexural vibration of a beam due to the presence of transverse cracks by using the Rayleigh-Ritz method. In this study, a beam with a single-sided crack or a pair of double-sided cracks was modeled as two separate beams divided by the crack. The equation of motion and associated boundary conditions have been derived by Shen and Pierre (1994) for a uniform Bernoulli-Euler beam containing one single-edge crack and the generalized variational principle used allows for modified stress, strain and displacement fields that satisfy the compatibility requirements in the vicinity of the crack. Chati *et al.* (1997) have studied the modal analysis of a cantilever beam with a transverse edge crack. The opening and closing cracks were considered. Chondros *et al.* (1998) have developed a continuous cracked beam vibration theory for the lateral vibration of cracked Euler-Bernoulli beams with single-edge or double-edge open cracks. The Hu-Washizu-Barr variational formulation was used to develop the differential equation and the boundary conditions of the cracked beam as a one-dimensional continuum. Saavedra and Cuitino (2001) presented a theoretical and experimental dynamic behavior of different multi-beam systems containing transverse cracks. Kishen and Kumar (2004) studied fracture the behavior of cracked beam-columns, by using the finite element method and the beam-column element. Karaagac *et al.* (2009) have investigated the effects of crack ratios and positions on the fundamental frequencies and buckling loads of slender cantilever Euler beams with a single-edge

crack both experimentally and numerically, using the finite element method, based on energy approach. Sekhar (1999) has presented the Finite Element (FEM) analysis of a rotor system for flexural vibrations by including a shaft with two open cracks and the influence of one crack over the other for eigenfrequencies, mode shapes and for threshold speed limits has been observed. Zheng and Kessissoglou (2004) have studied the natural frequencies and mode shapes of a cracked beam using the finite element method. An "overall additional flexibility matrix", instead of the "local additional flexibility matrix", was added to the flexibility matrix of the corresponding intact beam element to obtain the total flexibility matrix, and therefore the stiffness matrix. Yokoyama and Chen (1998) have investigated the vibration characteristics of a uniform Bernoulli-Euler beam with a single edge crack using a modified line-spring model. Nikolakopoulos *et al.* (1991) have examined the problem of crack depth and position identification in one-bay frame structures using eigenfrequency measurements. The dynamical response of cracked concrete structures modeled as bilinear SDOF dynamical systems has been studied by Pandey and Benipal (2011). In this study, the dynamical behaviour of Model-I and Model- III subjected to sinusoidal loading has been investigated by using the techniques of nonlinear dynamical systems theory. Lu and Liu (2012) have presented a composite element method (CEM) to analyze the free and forced vibrations of a cracked Euler-Bernoulli beam with axial force.

As seen from aforementioned references, all studies are related to the uncracked frames. The effects of cracks on the dynamic behaviors of beams have been the subject of many investigations. Unfortunately, literature research reveals that much less study investigating the static and dynamic behaviours of cracked frames is present in the published literature.

In this work, the effects of crack depth and crack location on the in-plane free vibration cracked frame structures have been investigated numerically by using The Finite Element Method. For the rectangular cross-section beam, a crack element is developed by using the principles of fracture mechanics. The effects of crack depth and location on the first two natural frequencies of multi-bay and multi-store frame structures are presented in 3D graphs. The comparison between the present work and the results obtained from ANSYS shows a very good agreement.

2. The local flexibility due to the crack

A crack on a beam introduces considerable local flexibility due to the strain energy concentration in the vicinity of the crack tip under load. The idea of an equivalent spring i.e. a local compliance is used to quantify, in a macroscopic way, the relation between the applied load and the strain concentration around the tip of the crack (Karaagac *et al.* 2009). A beam element of rectangular cross-section has an edge crack with a tip line parallel to the *z*-axis, i.e., with a uniform depth. A generalized loading is indicated by three general forces: an axial force P_1, shear force P_2 and bending moment P_3 as seen in Fig. 1(a).

In this work, the cross section of the beam is assumed to be rectangular. The additional strain energy due to the existence of a crack can be expressed as (Karaagac *et al.* 2009, Zheng and Kessissoglou 2004)

$$\Pi_c = \int_{A_c} G dA \qquad (1)$$

where *G* is the strain energy release rate function and A_c is the effective cracked area. The strain energy release rate function *G* can be expressed as (Zheng and Kessissoglou 2004)
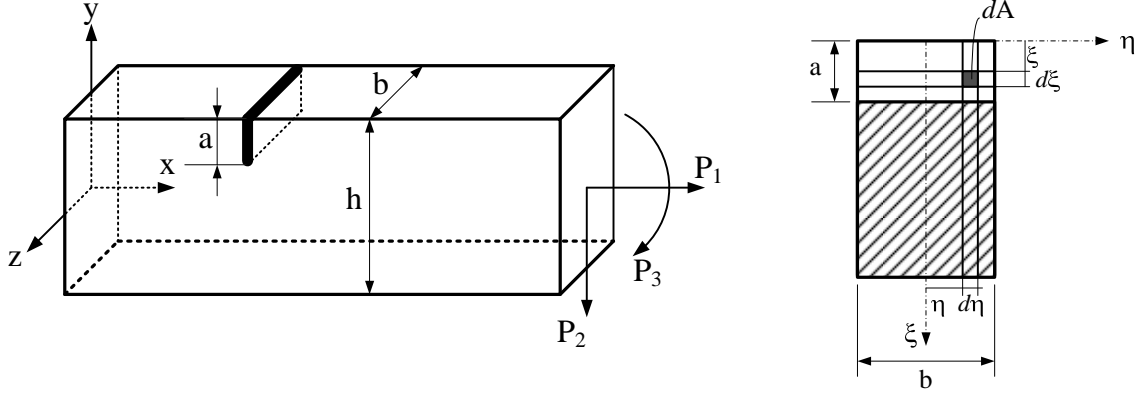
Fig. 1(a) Schematic view of a cracked beam under generalized loading conditions; (b) Geometry of cracked section showing integral limits

$$G = \frac{1}{E'}\left[(K_{I1} + K_{I2} + K_{I3})^2 + K_{II1}{}^2\right] \tag{2}$$

where $E' = E$ for plane stress problem, $E' = E/(1 - \mu^2)$ for plane strain problem (Karaagac *et al.* 2009, Zheng and Kessissoglou 2004). K_{In} and K_{IIn} (n = 1, 2, 3) are the stress intensity factors of the two modes of fracture (opening and sliding types) corresponding to generalized loading P_n, respectively. The stress intensity factor K_{I2} is ignored (Shen and Pierre 1994).

$$K_{I1} = \frac{P_1}{bh}\sqrt{\pi\xi}\,F1\left(\frac{\xi}{h}\right), \; K_{I3} = \frac{6P_3}{bh^2}\sqrt{\pi\xi}\,F2\left(\frac{\xi}{h}\right), \; K_{II2} = \frac{P_2}{bh}\sqrt{\pi\xi}\,F3\left(\frac{\xi}{h}\right) \tag{3}$$

where

$$F1(s) = \sqrt{\frac{\tan\left(\frac{\pi s}{2}\right)}{\left(\frac{\pi s}{2}\right)}} \; \frac{0.752 + 2.02s + 0.37\left(1 - \sin\left(\frac{\pi s}{2}\right)\right)^3}{\cos\left(\frac{\pi s}{2}\right)} \tag{4}$$

$$F2(s) = \sqrt{\frac{\tan\left(\frac{\pi s}{2}\right)}{\left(\frac{\pi s}{2}\right)}} \; \frac{0.923 + 0.199\left(1 - \sin\left(\frac{\pi s}{2}\right)\right)^4}{\cos\left(\frac{\pi s}{2}\right)} \tag{5}$$

$$F3(s) = \frac{1.122 - 0.561s + 0.085s^2 + 0.018s^3}{\sqrt{1 - s}} \tag{6}$$

Fn(s = ξ/h) represents the correction function which takes into account finite dimensions of the beam and takes particular forms for different geometry and loading modes. It is worth noting that *a*

is the final crack depth while ξ is the crack depth during the process of penetration from zero to the final depth.

The elements of the overall additional flexibility matrix c_{ij} can be expressed as (Karaagac *et al.* 2009, Zheng and Kessissoglou 2004).

$$c_{ij} = \frac{\partial \delta_i}{\partial P_i} = \frac{\partial^2 \Pi_C}{\partial P_i \partial P_j} \ (i, j = 1, 2, 3...) \tag{7}$$

Substituting Eqs. (3)-(6) in Eq. (7) yields the general equation for the local compliances as follows (considering that all K's are independent of η; η: see Fig. 1(b))

$$c_{ij} = \frac{b}{E'} \frac{\partial^2}{\partial P_i \partial P_j} \int_0^a \left\{ \left[\frac{P_1}{bh} \sqrt{\pi\xi} F1\left(\frac{\xi}{h}\right) + \frac{6P_3}{bh^2} \sqrt{\pi\xi} F2\left(\frac{\xi}{h}\right) \right]^2 + \frac{P_2^2}{b^2 h^2} \pi\xi F3^2\left(\frac{\xi}{h}\right) \right\} d\xi \tag{8}$$

$$(\ i, j = 1, 2, 3,...)$$

where c_{ij} is the local flexibility matrix

$$c_{ij} = \begin{bmatrix} c_{11} & c_{12} & c_{13} \\ c_{21} & c_{22} & c_{23} \\ c_{31} & c_{32} & c_{133} \end{bmatrix} \tag{9}$$

3. The crack finite element model

A finite element model is developed to represent a cracked beam element of length d and the crack is located at a distance d_1 from the left end of the element as shown in Fig. 2.

The element is then considered to be split into two segments by the crack. The left and right segments are represented by non-cracked sub elements. The crack represents net ligament effect created by loadings. This effect can be related to the deformation of the net ligament through the compliance expressions (c_{ij}) by replacing the net ligament with a fictitious spring connecting both faces of the crack (Yokoyama and Chen 1998).

The spring effects are introduced to the system by using the local flexibility matrix given by Eq. (9). The cracked element has 2 nodes with three degrees of freedom in each node. They are denoted as lateral bending displacements (v_1, v_2), slopes (v_1', v_2'), and longitudinal displacements (u_1, u_2).

For $0 \le x \le d_1$

$$v_1(x) = a_1 + a_2 x + a_3 x^2 + a_4 x^3$$
$$v_1' = \frac{dv_1}{dx}, \ u_1(x) = b_1 + b_2 x \tag{10a}$$

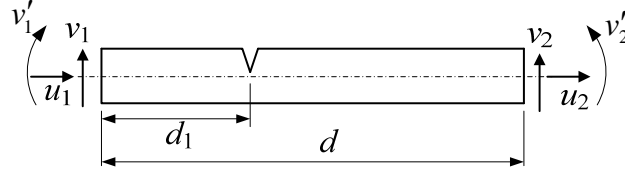For $d_1 \le x \le d$

Ahmed M. Ibrahim, Hasan Ozturk and Mustafa Sabuncu

Fig. 2 Crack Locations in crack element

$$v_2(x) = a_5 + a_6 x + a_7 x^2 + a_8 x^3$$
$$v_2' = {dv_2}\big/{dx}, \quad u_2(x) = b_3 + b_4 x \tag{10b}$$

The coefficients *a* and *b* of the polynomials can be expressed uniquely in terms of the boundary conditions and the local flexibility concept at the crack location. Eventually, the following expressions are obtained for a cracked element:

For lateral bending

$$v_1(0) = q_1 , \quad v_1'(0) = q_2$$
$$v_2(d) = q_3 , \quad v_2'(d) = q_4 \tag{11a}$$

Longitudinal displacement

$$u_1(0) = q_5 , \quad u_2(d) = q_6 \tag{11b}$$

At the crack location d_1, the flexibility concept requires:
For lateral bending:
Continuity of the vertical displacement

$$v_1(d_1) = v_2(d_1) \tag{12a}$$

Discontinuity of the cross-sectional rotation (slope)

$$v_2'(d_1) = v_1'(d_1) + c_{33} M_1(d_1) \tag{12a}$$

where $M_1(d_1) = EIv_1'' \big|_{x=d_1}$
Continuity of bending moment

$$M_1(d_1) = M_2(d_1) \tag{12c}$$

Continuity of shear force

$$S_1(d_1) = S_2(d_1) \tag{12d}$$

For longitudinal displacement:
Discontinuity of longitudinal displacement
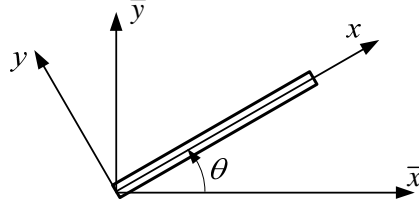
$$u_2(d_1) = u_1(d_1) + c_{11} T_1(d_1) \tag{13a}$$

Fig. 3 Transformations from local to global coordinates

where $T_1(d_1) = EAu_1'|_{x=d_i}$ Continuity of force

$$T_1(d_1) = T_2(d_1) \tag{13b}$$

By considering Eq. (10) describing the displacement for the left and right parts of the element and rearranging Eqs. (11)-(13), the nodal displacement can be expressed in matrix forms as

$$\{q_v\} = [D_v]\{a\}, \ \{q_u\} = [D_u]\{b\} \tag{14}$$

where

$$\begin{aligned} \{q_v\} &= [q_1 \quad q_2 \quad 0 \quad 0 \quad 0 \quad 0 \quad q_3 \quad q_4]^T \\ \{q_u\} &= [q_5 \quad 0 \quad 0 \quad q_6]^T \end{aligned} \tag{14a}$$

$$\begin{aligned} \{a\} &= [a_1 \quad a_2 \quad a_3 \quad a_4 \quad a_5 \quad a_6 \quad a_7 \quad a_8]^T \\ \{b\} &= [b_1 \quad b_2 \quad b_3 \quad b_4]^T \end{aligned} \tag{14b}$$

The generalized displacement vector according to local reference coordinates can be expressed as

$$q = [u_1 \quad v_1 \quad v_1' \quad u_2 \quad v_2 \quad v_2'] \tag{15}$$

As seen in Fig. 3, the relation between local and global reference coordinates can be written as

$$q = T\overline{q} \tag{16}$$

where *T* is the transformation matrix

$$T = \begin{bmatrix} \cos\theta & \sin\theta & 0 & 0 & 0 & 0 \\ -\sin\theta & \cos\theta & 0 & 0 & 0 & 0 \\ 0 & 0 & 1 & 0 & 0 & 0 \\ 0 & 0 & 0 & \cos\theta & \sin\theta & 0 \\ 0 & 0 & 0 & -\sin\theta & \cos\theta & 0 \\ 0 & 0 & 0 & 0 & 0 & 1 \end{bmatrix} \tag{17}$$

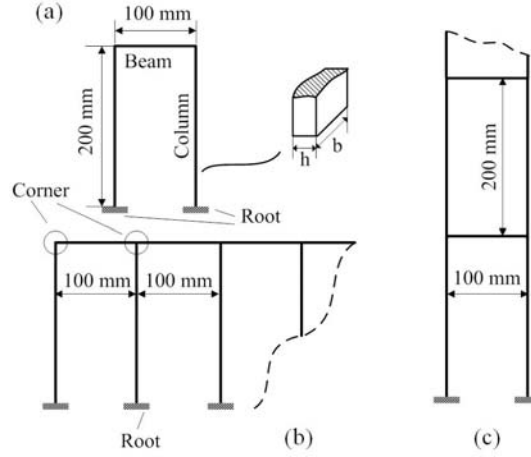Fig. 4 Frame structures, (a) one-bay frame; (b) multi-bay frame; (c) multi-story frame

4. Energy equations

Energy equations should be expressed separately from the crack element and intact elements on the left side of the crack element.
The elastic potential energy U:
For intact elements on the left side of the cracked element

$$U_L = \frac{1}{2}\left(\int_0^d EI(v_1'')^2\,dx\right) + \frac{1}{2}\left(\int_0^d EA(u_1')^2\,dx\right) \tag{18a}$$

For the cracked element

$$U_C = \frac{1}{2}\left(\int_0^{d_1} EI(v_1'')^2\,dx\right) + \frac{1}{2}\left(\int_0^{d_1} EA(u_1')^2\,dx\right) + \frac{1}{2}\left(\int_{d_1}^d EI(v_2'')^2\,dx\right) + \frac{1}{2}\left(\int_{d_1}^d EA(u_2')^2\,dx\right) \tag{18b}$$

For intact element on the right side of the cracked element

$$U_R = \frac{1}{2}\left(\int_0^d EI(v_2'')^2\,dx\right) + \frac{1}{2}\left(\int_0^d EA(u_2')^2\,dx\right) \tag{18c}$$

Similarly, the kinetic energy *T* of an element of length *d* in an Euler beam is given as follows for the intact elements on the left side of the cracked element

$$T_L = \frac{1}{2}\left(\int_0^a \rho A(\dot{v}_1^2 + \dot{u}_1^2)\,dx\right) \tag{19a}$$

For the cracked element

$$T_C = \frac{1}{2}\left(\int_0^{d_1} \rho A(\dot{v}_1^2 + \dot{u}_1^2)dx\right) + \frac{1}{2}\left(\int_{d_1}^{d} \rho A(\dot{v}_2^2 + \dot{u}_2^2)dx\right) \tag{19b}$$

For intact element on the right side of the cracked element

$$T_R = \frac{1}{2}\left(\int_0^{d} \rho A(\dot{v}_2^2 + \dot{u}_2^2)dx\right) \tag{19c}$$

In which the first and second terms represent the energies due to lateral and longitudinal motions, respectively.

5. Equation of motion

The elastic stiffness matrix $[k_e]$ and mass matrix $[m_e]$ are obtained for both cracked finite element and intact finite elements. Mass and stiffness matrices of each beam element are used to form global mass and stiffness matrices. By performing the required operations for the entire system, one obtains the following governing matrix equations giving natural frequency (ω).

$$([K] - \omega^2[M])\{\overline{q}\} = 0 \tag{20}$$

Where $[K]$ and $[M]$ represent global elastic stiffness and mass matrices, respectively.

Table 1 Properties of the frame structure

Properties		Quantity
Modulus of elasticity, E		200 GPa
Mass density, ρ		7900 kg/m^3
Cross-section	h	5 mm
	b	20 mm
Column length		200 mm
Beam length		100 mm

Table 2 Comparison between the present work and ANSYS results; The crack location is at the fixed point of the one-bay frame structure

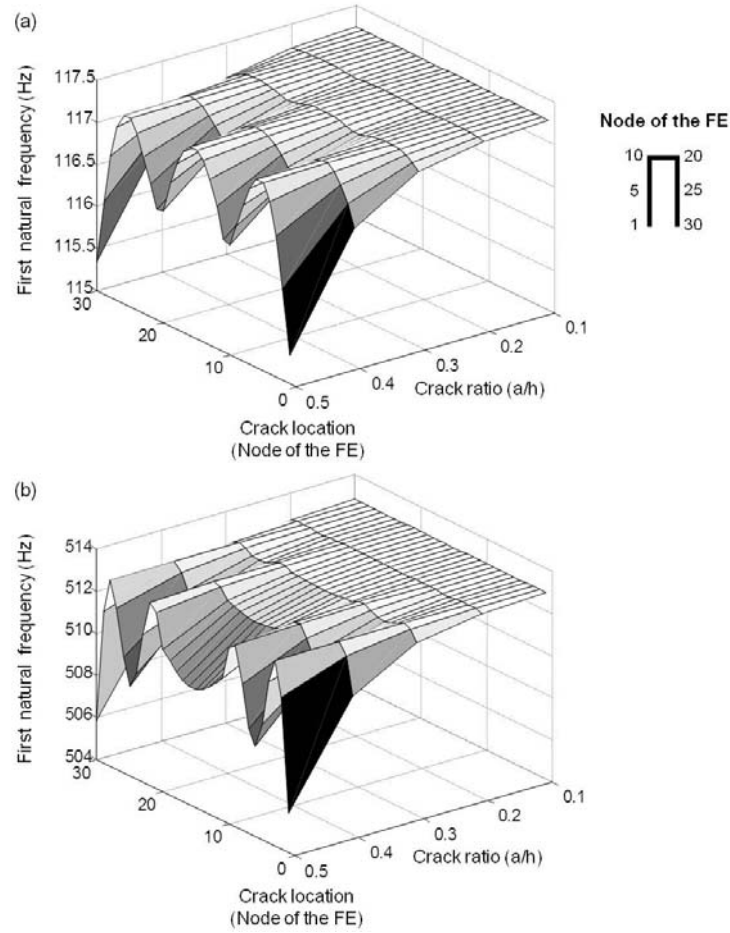| Crack (a/h)	ANSYS (Hz)	Present work (Hz)	ERROR%
0	118.555	117.2552	1.108522
0.1	118.356	117.2532	0.940545
0.2	117.726	117.2223	0.429685
0.3	116.648	117.0806	0.369526
0.4	115.006	116.6234	1.386837
0.5	112.594	115.3395	2.3804

Fig. 5 Crack effect on the natural frequencies of one-bay frame structure; (a) The first natural frequency; (b) The Second natural frequency
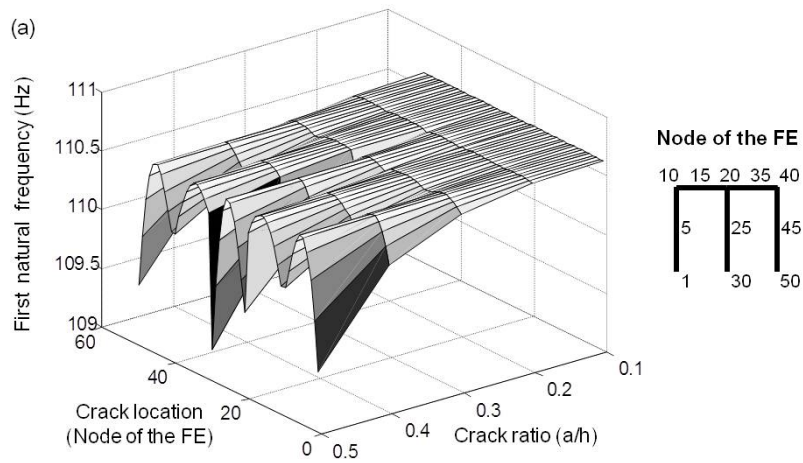

Fig. 6 Crack effect on the natural frequencies of a two-bay frame structure
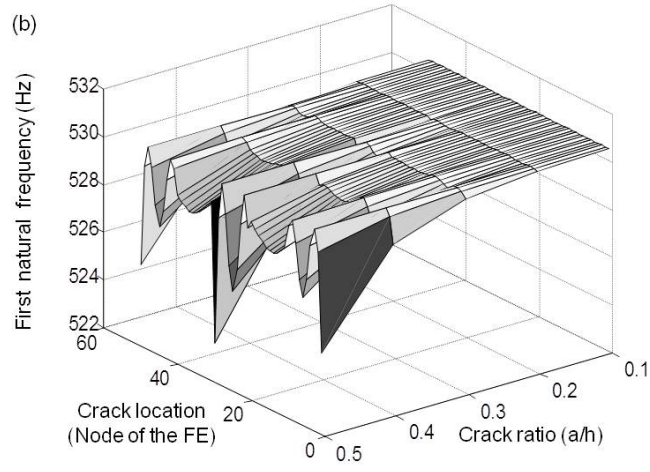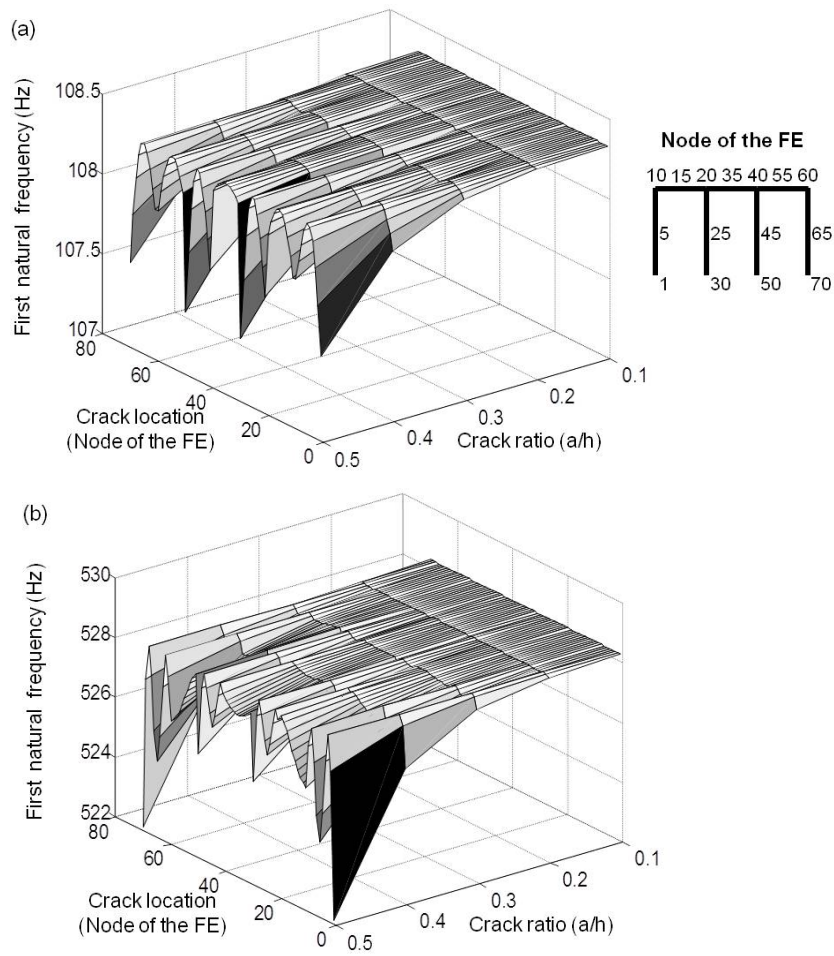
Fig. 6 Continued

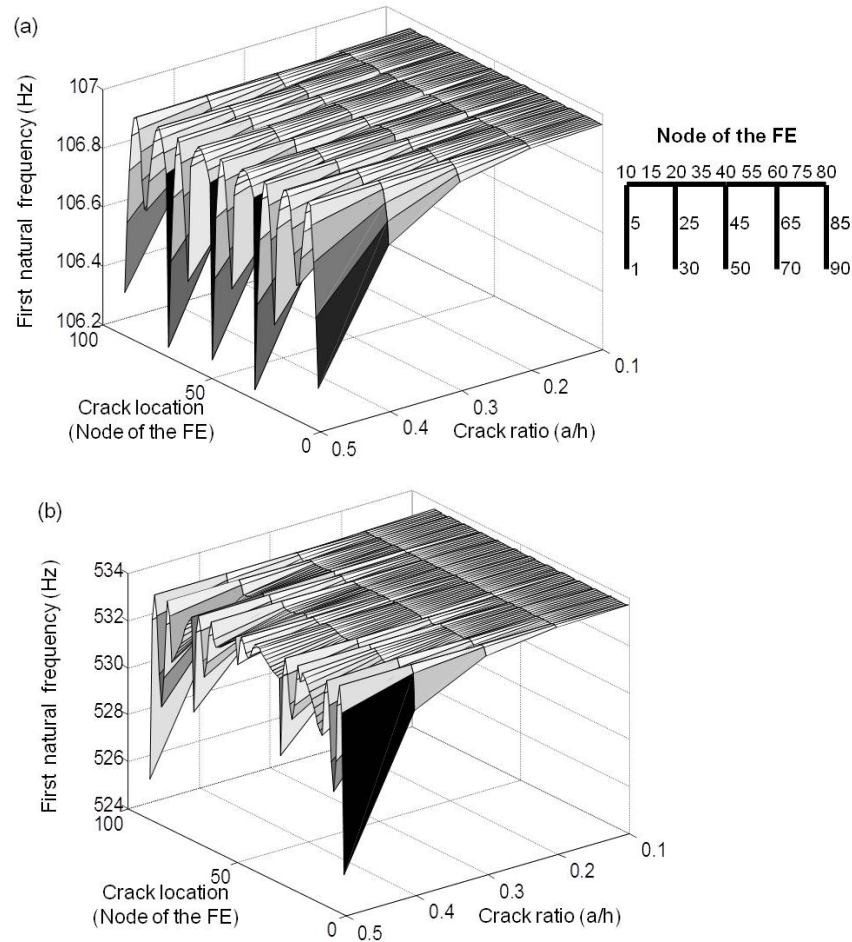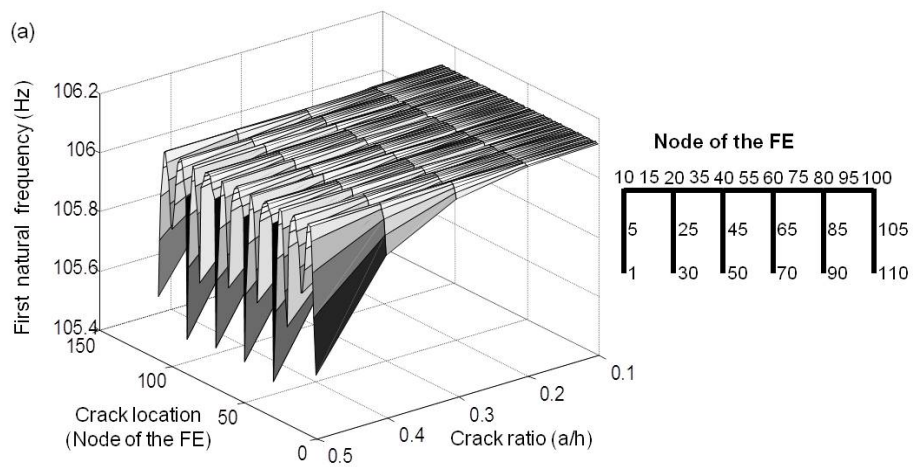Fig. 7 Crack effect on the natural frequencies of a three-bay frame structure

Ahmed M. Ibrahim, Hasan Ozturk and Mustafa Sabuncu

Fig. 8 Crack effect on the natural frequencies of a four-bay frame structure

Fig. 9 Crack effect on the natural frequencies of a five-bay frame structure
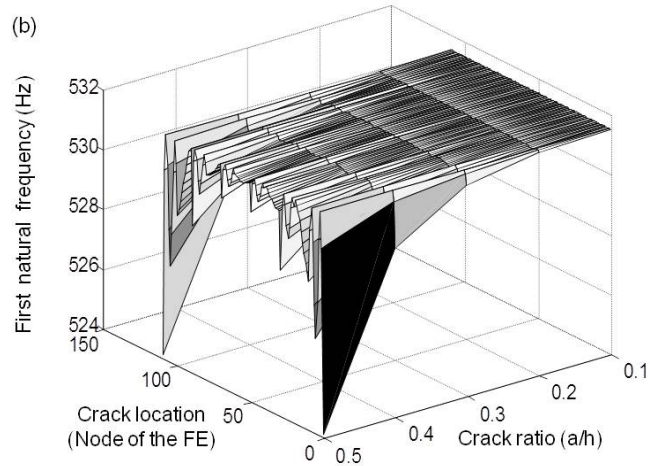
(b)

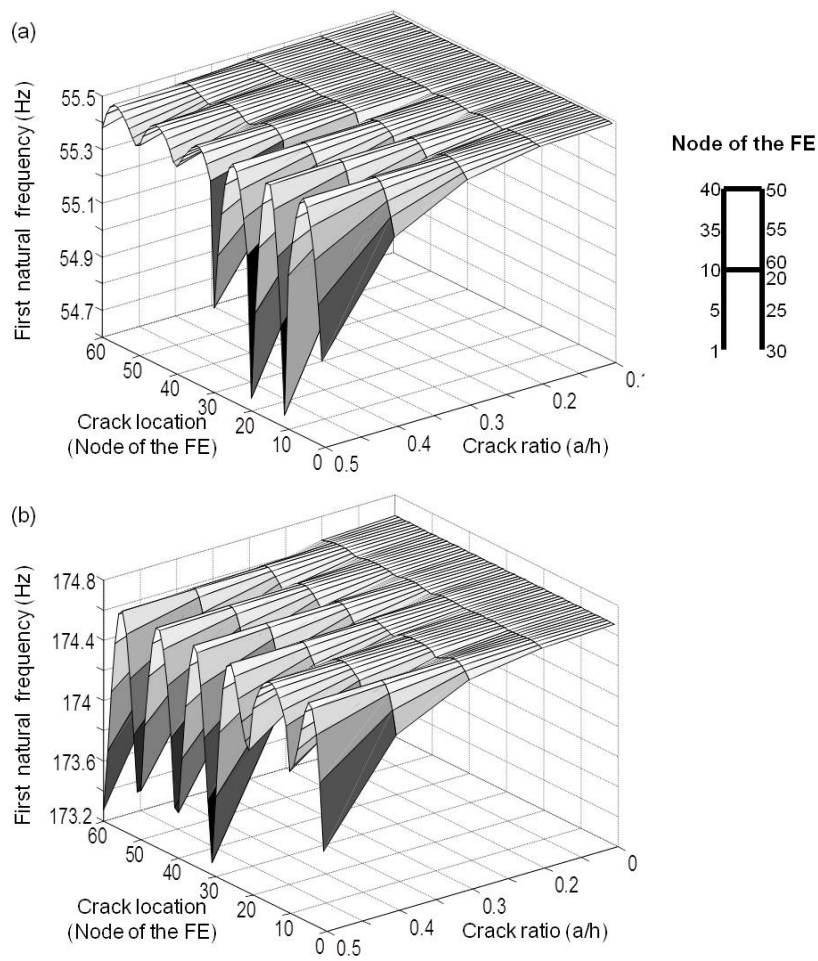Fig. 9 Continued

(a)

(b)

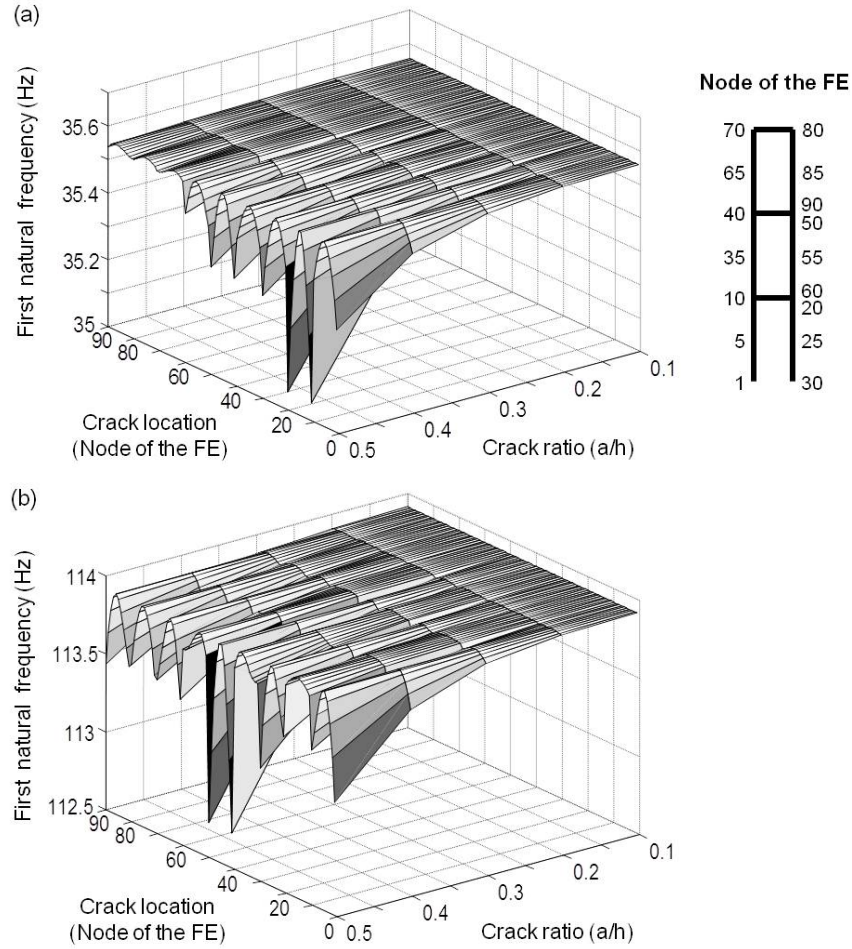Fig. 10 Crack effect on the natural frequencies of a two-story frame structure

Fig. 11 Crack effect on the natural frequencies of a three-story frame structure

6. Results comparison

In this study, the multi-bay and multi-store frames constituting of column and beam, having rectangular cross-sections are used, as seen in Fig. 4 and the dimensions and material properties are given in Table 1. Comparison have been made between the natural frequencies of cracked frames obtained using the present model with the results obtained from the ANSYS software. The modelling of crack in ANSYS is built by using the method of concentrate meshing around the crack location. By using KSCON (a command in ANSYS) a concentration key-point is defined about which the mesh area will be skewed. This is useful for modelling stress concentrations and crack tips. During meshing, elements are initially generated circumferentially about, and radially away, from the key-point. Lines attached to the key-point are given appropriate divisions and spacing ratios (Phan 2010).

As seen from Table 2, the maximum error is 2.3804%. The comparison shows that very good agreement obtained is between the results.

Table 3 Decreases in first natural frequency of the one-bay frame structure with respect to crack location when the crack ratio is 0.5

Crack location (nodes)	10th, 20th	1st, 30th	Without crack 117.23
Natural frequency (Hz)	116.3	115.33	
Percentage of decreases in the frequency	0.79%	1.62%	

Table 4 Decreases in first natural frequency of the two-bay frame structure with respect to crack location when the crack ratio is 0.5

Crack location (nodes)	10th, 40th	20th	1st, 50th	30th	Without crack 110.61
Natural frequency (Hz)	110.09	109.72	109.51	109.26	
Percentage of decreases in the frequency	0.47%	0.80%	0.99%	1.22%	

Table 5 Decreases in first natural frequency of the three-bay frame structure with respect to crack location when the crack ratio is 0.5

Crack location (nodes)	10th, 60th	20th, 40th	1st, 70th	50th, 30th	Without crack 108.32
Natural frequency (Hz)	107.93	107.73	107.53	107.39	
Percentage of decreases In the frequency	0.36%	0.54%	0.73%	0.86%	

Table 6 Decreases in first natural frequency of the four-bay frame structure with respect to crack location when the crack ratio is 0.5

Crack location (nodes)	10th, 80th	40th	20th, 60th	1st, 90th	50th	30th, 70th	10th, 80th	Without crack 106.96
Natural frequency (Hz)	106.66	106.53	106.49	106.34	106.26	106.23	106.66	
Percentage of decreases in the frequency	0.28%	0.40%	0.44%	0.58%	0.65%	0.68%	0.28%	

Table 7 Decreases in first natural frequency of the five-bay frame structure with respect to crack location when the crack ratio is 0.5

Crack location (nodes)	10th, 100th	40th, 60th	20th, 80th	1st, 110th	50th, 70th	30th, 90th	Without crack 106.11
Natural frequency (Hz)	105.86	105.72	105.72	105.61	105.53	105.51	
Percentage of decreases in the frequency	0.24%	0.37%	0.37%	0.47%	0.55%	0.57%	

6.1 Multi-bay frame structures

Figs. 5(a), 6(a), 7(a), 8(a) and 9(a) show the effect of crack location and crack depth on the first natural frequencies of frame structures having one, two, three, four and five. As the crack depth increases, the variations of the first natural frequency become significant.

As seen in Figs. 5(a), 6(a), 7(a), 8(a) and 9(a) for a/h=0.5, when the crack location changes, the variations in the first natural frequencies of one, two, three, four and five bay frame structures are centered symmetrically around the 15th, 25th (except for the region between the 20th and 30th nodes), 35th, 45th (except for the region between the 40th and 50th nodes) and 55th nodes of the FE, respectively.

The maximum decreases in the first natural frequencies occur when the crack is at the fixed points (roots of the frame), the 30th node (root of the middle column), the 30th and 50th nodes (roots of the internal columns), the 30th and 70th nodes (roots of the second and fourth columns), the 30th and 90th nodes (roots of the second and fifth columns) respectively for one, two, three, four and five bay frame structures. These are about 1.62%, 1.22%, 0.86%, 68% and 0.57% with respect to the frequency of the frame without crack. Moreover, the crack does not affect the first natural frequency of the multi-bay frames structure when it is located at the particular points of the column and the beam lengths, since the stresses in these points are so small.

Figs. 5(b), 6(b), 7(b), 8(b) and 9(b) show the effect of crack location and crack depth on the second natural frequencies of frame structures having one, two, three, four and five bays. As seen in Figs. 5(b), 6(b), 7(b), 8(b) and 9(b), similar to the effect of the crack on the first natural frequency, the left and the right hand side of the results obtained from maximum crack depth condition around the 15th, 25th (except for the region between the 20th and 30th nodes), 35th, 45th (except for the region between the 40th and 50th nodes) and 55th nodes of the FE are symmetric respectively for one, two, three, four and five bay frame structures.

The maximum decreases in the second natural frequencies occur when the crack is at the fixed points (roots of the frame), the 30th node (root of the middle column), the 1st and 70th nodes (roots of the external columns), the 1st and 90th nodes (roots of the first and fifth columns), the 1st and 110th nodes (root of the external columns) respectively for one, two, three, four and five bay frame structures.
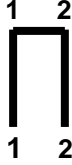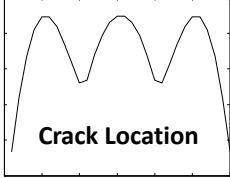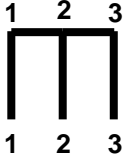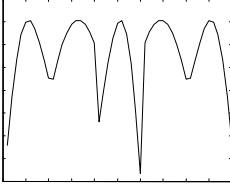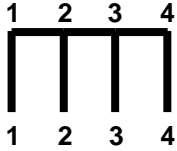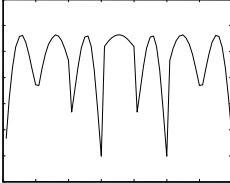
6.2 Two-story frame structure

Fig. 10(a) shows the effect of crack location and crack depth on the first natural frequency of the two-story frame structure. As the cr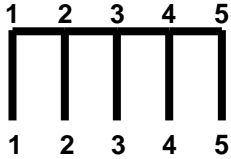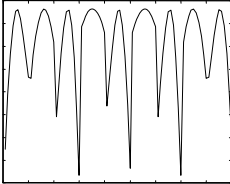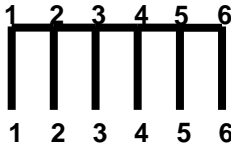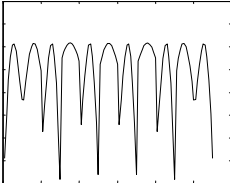ack depth increases, variation of the first natural frequency becomes significant. When the crack location changes, variation in the first natural frequency between the 1st and 30th nodes is centered symmetrically around the 15th node. On the other hand, the changes of frequency when the crack is between the 30th and 60th nodes is centered symmetrically around the 45th node of the FE as seen in Fig. 10(a) for a/h = 0.5. The maximum decrease in the first natural frequency occurs when the crack is at the 10th and 20th nodes (the joint point between the lower and the upper frame when the stresses due to the moment become maximum).

Fig. 10(b) shows the effect of crack location and crack depth on the second natural frequency of the two-story frame structure. As seen in Fig. 10(b), similar to the effect of crack on the first natural frequency, the left and the right hand side of the results obtained from the maximum crack depth is symmetric when the crack is between the 1st and 30th nodes. There is also similar symmetry between the 30th and 60th nodes. The maximum decrease in the second natural frequency occurs when the crack is at the joint point between the lower and the upper frame at the 30th and 60th nodes. Moreover, decreases in the second natural frequency also exist when the crack is at the 1st, 10th, 20th, 40th and 50th nodes.

Table 8 Location of maximum decrease in the first natural frequencies in multi-bay frames

Frames	Frequency at the crack ratio 0.5 (see Figs. 5(a)-9(a))	Location of Max. decrease in roots	Location of Max. decrease in corners
One-bay	ω_1 (Hz) **Crack Location**	1,2	1,2
Two-bay	ω_1 (Hz)	2	2
Three-bay	ω_1 (Hz)	2,3	2,3
Four-bay	ω_1 (Hz)	2,4	2,4
Five-bay	ω_1 (Hz)	2,5	2,5
n: number of columns		2 , n-1	2 , n-1

6.3 Three-story frame structure

Fig. 11(a) shows the effect of crack location and crack depth on the first natural frequency of the three-story frame structure. As the crack depth increases, variation of the first natural frequency becomes significant. When the crack location changes, the variation in the first natural

frequency when the crack is between the 1st and 30th nodes is centered symmetrically around the 15th node. There is the similar symmetry in the area between the 30th and 60th nodes, and the area between the 60th and 90th nodes of the FE as seen in the Figure. The maximum decrease in the first natural frequency occurs when the crack is at the 10th and 20th nodes (the joint point between the lower and the middle frame where the stresses due to the moment become maximum). Decreases in the frequency also occur when crack is at the 1st and 30th nodes (the roots of the frame) and when the crack is at 40th, 50th, 60th, 70th, 80th and 90th nodes.

Fig. 11(b) shows the effect of crack location and crack depth on the second natural frequency of the three-story frame structure. As seen in the Figure, similar to the effect of the crack on the first natural frequency, the variation in the second natural frequency when the crack is between the 1st and 30th nodes is centered symmetrically around the 15th node, there is a similar symmetry centered around the 45th and 75th crack nodes for the area between the 30th and 60th, 60th and 90th nodes of the FE, respectively. The maximum decrease in the second natural frequency occurs when the crack is at the joint point between the middle and upper frame at the 40th and 50th nodes. Moreover, decreases in the second natural frequency also exist when the crack is at the 1st, 10th, 20th, 30th, 60th, 70th, 80th and 90th nodes.

7. Assessment of vibration analysis for the multi-bay frame structure

When the results obtained from the free vibration analysis of multi-bay frames, shown in Figs. 5(b), 6(b), 7(b), 8(b) and 9(b), are examined, generally the first natural frequencies decrease when the crack is located either at the roots or at the corner of the frames for all multi-bay frames. Crack location, first natural frequencies of the cracked structure, percentage of decreases and the first natural frequencies without crack are given in Tables 3-7. In these tables, percentage decrease in the first natural frequencies is calculated with respect to the maximum decrease. As seen in Tables 3-7, the maximum decreases in the first natural frequency of the multi-bay frames occur, if the crack is located at the roots of the 2nd column or n-1 number of column and at the corner of the 2nd column or n-1 number of column (n: number of columns). In other words, it is observed that the locations of maximum decrease in the first natural frequency depend on the particular formulation. This formulation is given schematically in Table 8. This phenomenon is not observed for the second natural frequency, since, the second mode shapes do not have a similar form as the first mode shapes.

8. Conclusions

In this study, the effects of crack depth and crack location on the in-plane free vibration of cracked frame structures have been investigated numerically by using the Finite Element Method. For the rectangular cross-section beam, a crack element is developed by using the principles of fracture mechanics. The following conclusions are drawn.

- The reduction of natural frequency depends on the crack depth and crack location.
- Higher drops in the in-plane natural frequency are observed when the crack is located near the roots or corners of the frames.
- When the number of columns increases in the multi-bay frame structures, the effect of the crack decreases on the natural frequencies.

- The locations of maximum decreases in the first natural frequency of the multi-bay frames depend on the particular formulation.
- There is no effect of the crack on the in-plane natural frequency when the crack is located at the nodal points of the mode shape.

References

Bayo, E. and Loureiro, A. (2001), "An efficient and direct method for buckling analysis of steel frame structures", *J. Constr. Steel. Res.*, **57**, 1321–36.

Chang, G.S. and Chang, C.H. (1991), "Out-of-plane vibrations of plane frames", *J. Sound. Vib.*, **147**(1), 137-54.

Chati, M., Rand, R. and Mukherjee, S. (1997), "Modal analysis of a cracked beam", *J. Sound. Vib.*, **207**(2), 240-70.

Chondros, T.G. and Dimarogonas, A.D. (1989), "Dynamic sensitivity of structures to cracks", *J. Vib. Acoust. Stress Reliab. Des.*, **111**, 251-56.

Chondros, T.G., Dimarogonas, A.D. and Yao, J. (1998), "A continuous cracked beam vibration theory", *J. Sound. Vib.*, **215**, 17–34.

Christides, S. and Barr, A.D.S. (1984), "One-dimensional theory of cracked Bernoulli-Euler beams", *Int. J. Mech. Sci.*, **26**(11-12), 639-48.

Filipich, C.P. and Laura, P.A.A. (1987), "In-plane vibrations of portal frames with end supports elastically restrained against rotation and translation", *J. Sound. Vib.*, **117**(3), 467-73.

Filipich, C.P., Ercoli, L., Laura, P.A.A., Rossi, R.E. and Herrera, R. (1989), "Analytical and experimental investigation on vibrating frames carrying concentrated masses", *Appl. Acoust.*, **26**, 243-50.

Girgin, K., Ozmen, G. and Orakdogen, E. (2006), "Buckling lengths of irregular frame columns", *J. Constr. Steel. Res.*, **62**(6), 605-613.

Gounaris, G. and Dimarogonas, A. (1988), "A finite element of a cracked prismatic beam for structural analysis", *Comput. Struct.*, **28**(3), 309-13.

Gupta, KK. (1970), "Vibration of frames and other structures with banded stiffness matrix", *Int. J. Numer. Meth. Eng.*, **2**, 221-28.

Karaagac, C., Ozturk, H. and Sabuncu, M. (2009), "Free vibration and lateral buckling of a cantilever slender beam with an edge crack: Experimental and numerical studies", *J. Sound. Vib.*, **326**(1-2), 235-50.

Kishen, J.M.C. and Kumar, A. (2004), "Finite element analysis for fracture behavior of cracked beam-columns", *Finite. Elem. Anal. Des.*, **40**(13-14), 1773-89.

Laurai, P.A.A., Valerga, De., Greco, B. and Filipich, CP. (1987), "In-Plane vibrations of frames carrying concentrated masses", *J. Sound. Vib.*, **117**(3), 447-58.

Lee, H.P. (1993), "Natural frequencies and modes for the in-plane vibration of a triangular closed frame", *J. Sound. Vib.*, **167**(3), 568-72.

Lee, H.P. and Ng, T.Y. (1994), "In-plane vibration of planar frame structures", *J. Sound. Vib.*, **172**(3), 420-27.

Lee, H.P. and Ng, T.Y. (1994), "Natural frequencies and modes for the flexural vibration of a cracked beam", *Appl. Acoust.*, **42**(2), 151-63.

Lu, Z.R. and Liu, J.K. (2012), "Vibration analysis of a cracked beam with axial force and crack identification", *Smart. Struct. Syst.*, **9**(4), 355-371.

Nikolakopoulos, P.G., Katsareas, D.E. and Papadopoulost, C.A. (1991), "Crack identification in frame structures", *Comput. Struct.*, **64**(14), 389-406.

Ostachowicz, W.M. and Krawczuk, M. (1990), "Vibration analysis of a cracked beam", *Comput. Struct.*, **36**(2), 245-50.

Pandey, U.K. and Benipal, G.S. (2011), "Bilinear elastodynamical models of cracked concrete Beams", *Struct. Eng. Mech.*, **39**(4), 465-498.

Phan, A.V. (2010), "ANSYS TUTORIAL–2-D Fracture Analysis ANSYS Release 7.0", University of South Alabama.

Qian, G.L., Gu, S.N. and Jiang, J.S. (1990), "The dynamic behaviour and crack detection of a beam with a crack", *J. Sound. Vib.*, **138**(2), 233-43.

Saavedra, P.N. and Cuitino, L.A. (2001), "Crack detection and vibration behavior of cracked beams", *Comput. Struct.*, **79**, 1451–59.

Sekhar, A.S. (1999), **"**Vibration characteristics of a cracked rotor with two open cracks", *J. Sound. Vib.*, **223**(4), 497-512.

Shen, M.H.H. and Pierre, C. (1994), *"*Free Vibrations of beams with a single-edge crack", *J. Sound. Vib.*, **170**(2), 237-59.

Syngellakis, S. and Kameshki, ES. (1994), "Elastic critical loads for plane frames by transfer matrix method", *J. Struct. Eng-ASCE.*, **120**(4), 1140-57.

Tong, GS. and   Xing, GR. (2007), "Determination of buckling mode for braced elastic–plastic frames", *Eng. Struct.*, **29**, 2487–96.

Trahair, N.S. (2009), "Buckling analysis design of steel frames", *J. Constr. Steel. Res.*, **65**(7), 1459-63.

Xu, L. and Liu, Y. (2002), "Story stability of semi-braced steel frames", *J. Constr. Steel. Res.*, **58**, 467–91.

Yokoyama, T. and Chen, MC. (1998), "Vibration analysis of edge-cracked beams using a line-spring model", *Eng. Fract. Mech.*, **59**(3), 403-9.

Zheng, D.Y. and Kessissoglou, N.J. (2004), "Free vibration analysis of a cracked beam by finite element method", *J. Sound. Vib.*, **273**, 457-75.